ELSEVIER

Coordination Chemistry Reviews
200–202 (2000) 887–900

COORDINATION CHEMISTRY REVIEWS

www.elsevier.com/locate/ccr

Flash and continuous photolysis studies of Roussin's red salt dianion $Fe_2S_2(NO)_4^{2-}$ in solution

James L. Bourassa, Peter C. Ford *

Department of Chemistry, University of California, Santa Barbara, CA 93106-9510, USA

Received 9 July 1999; accepted 7 January 2000

Contents

Abstract

Flash photolysis studies of Roussin's red salt dianion, $Fe_2S_2(NO)_4^{2-}$ (**RRS**) demonstrated high quantum yield formation of an intermediate believed to be $Fe_2S_2(NO)_3^{2-}$ formed by photodissociation of NO. This species reacts competitively with nitric oxide via second-order kinetics ($k_{NO} = 9.1 \times 10^8$ M^{-1} s^{-1}) to reform **RRS** and with dioxygen ($k_{Ox} = 5.6 \times 10^7$ M^{-1} s^{-1}) to give a secondary intermediate. The latter species is the likely precursor of the eventual photoproduct, Roussin's black salt anion, $Fe_4S_3(NO)_7^-$ (**RBS**). In deaerated aqueous solution, photolysis of the red salt also leads to formation of **RBS** but with a quantum yield (0.0039) much smaller than that in aerated solution (0.14). Notably, under these conditions N_2O is also found to be a product. In deoxygenated aprotic media, a different photoproduct, the black salt dianion $Fe_4S_3(NO)_7^{2-}$ is formed in low yield. The independently prepared dianion $Fe_4S_3(NO)_7^{2-}$ was shown to reduce NO to N_2O in the

* Corresponding author. Tel.: +1-805-893 2443; fax: +1-805-893 4120.
E-mail address: ford@chem.ucsb.edu (P.C. Ford).

PII: S0010-8545(00)00259-9

presence of a proton source. A scheme for the observed photochemistry of **RRS** based on these observations is proposed.

Keywords: Flash photolysis; Continuous photolysis; Roussin's red salt dianion

1. Introduction

A previous study in this laboratory centered on nitric oxide generation by the photolysis of the Roussin's red salt dianion (**RRS**), $[Fe_2S_2(NO)_4]^{2-}$ in aqueous aerated solutions [1]. The quantum yield for **RRS** disappearance proved to be substantial ($\Phi_{RRS} = 0.14 \pm 0.1$ mol einstein^{-1}) and the iron containing product was identified as the Roussin's black salt anion, $Fe_4S_3(NO)_7^-$ (**RBS**) in the stoichiometry shown in Eq. (1). The **RBS** formation was accompanied by equimolar formation of NO determined electrochemically [2]. Electrospray mass spectral evidence pointed to sulfide ion formation as well.

$$2Fe_2S_2(NO)_4^{2-} \xrightarrow{h\nu,\ \phi_{RRS}} Fe_4S_3(NO)_7^- + NO + S^{2-} + [e^-] \quad (1)$$

In this context, $Fe_2S_2(NO)_4^{2-}$ was examined as a precursor for photochemical NO generation to exploit the known nitric oxide sensitization of γ-radiation induced cell killing [3]. Hypoxic V79 cell cultures that were treated with **RRS** solution (0.75 mM) then subjected to γ-radiation (15 Gy) demonstrated strikingly lower survival rates when simultaneously exposed to white light irradiation than did control systems treated identically but not exposed to light [1]. These experiments provided an important proof-of-concept of photochemical strategies for NO delivery to biological targets.

In our earlier report, qualitative flash photolysis studies noting the formation of several transient species from **RRS** were described. At that time it appeared that the instability of **RRS** solutions under excess NO precluded quantitative evaluation of these intermediates. Here we report flash photolysis results using modified procedures that provide the opportunity for more detailed evaluation of the reactivities of key transients with NO and O_2.

It was also noted in our earlier report [1] that the quantum yields of concomitant **RRS** depletion and **RBS** formation are dependent on the presence of dioxygen in solution. In deaerated aqueous solutions, the red salt anion still undergoes photoconversion to **RBS**, but Φ_{RRS} was found to decrease to 0.0039. The residual photochemistry seen was attributed to NO itself serving as the necessary oxidant as evidenced by the qualitative observation of N_2O as a photoreaction product. The present study also addresses quantitative aspects of the photoreactivity under deaerated conditions.

2. Experimental section

Acetonitrile was distilled under dinitrogen from CaH_2 and used promptly. Water for spectroscopic and photochemical studies was purified by a Millipore system. Methanol was distilled under N_2 from iodine and Mg while ethanol was used as received from Quantum Chemical Corporation. Chromatographic grade argon (Air Liquide), used for deaerating solutions, was first passed through a Chromatograph Research Supplies oxygen trap. Nitric oxide (99.0%, Matheson) was passed through an Ascarite II® column to remove higher nitrogen oxides. The NO delivery system used only stainless steel tubing and fittings, and vacuum manifold connection was accomplished by a stainless steel-to-glass fitting. The synthesis of $Na_2[Fe_2S_2(NO)_4]\cdot 8H_2O$ was that described by Seyferth et al. [4].

Infrared (IR) spectra were obtained with a BioRad FTS 60 SPC 3200 FTIR spectrometer. Low temperature FTIR spectra were recorded using a PFD-FT12.5 fixed temperature Pourfill Dewar by R.G. Hansen and Associates and a sample IR cell built by the UCSB Machine Shop. UV–vis spectra were obtained with either a HP8572 diode array spectrometer or a Cary 118 spectrophotometer modernized by OLIS.

UV–vis absorption spectra and photolysis experiments under deaerated conditions employed 1 cm pathlength, 3.0 ml volume quartz cells fitted with glass stopcocks via Viton o-ring joints. The precise volume of each cell was determined by weighing before and after filling with water. Deaeration of solutions was achieved with three to five freeze–pump–thaw (f-p-t) cycles on a vacuum manifold. Continuous (CW) photolysis experiments were performed on optical trains using UVP 200 W Hg lamps with a 0.6 cm diameter beam and the appropriate interference filters as the excitation source [5]. Chemical actinometry was performed with ferric oxalate [6]. Solutions were stirred continuously during photolysis, and exposure to extraneous light was avoided. Quantum yield measurements were carried out under conditions designed to minimize thermal reactions ($< 2\%$), for which corrections were made.

Gas chromatography was carried out using a 5830A gas chromatograph fitted with a 12 ft, 80–100 mesh Porapak Q column at 140°C. NO retention times were similar to those of N_2, appearing at 1.27 min after injection, while N_2O appeared 2.07 min after injection and Ar, used as the internal standard, appeared at 1.86 min. Known samples of 10% N_2O in Ar were used to calibrate the GC.

Flash photolysis experiments were carried out with a time-resolved optical (TRO) apparatus using the third harmonic (355 nm) of a Nd:YAG ns pulse laser (Continuum NY60-20) as the excitation source, attenuated to ca. 10–30 mJ pulse^{-1} [7]. The probe source was a high pressure Xe lamp, and kinetic traces at single monitoring wavelengths (λ_{mon}) were recorded using a SPEX Doublemate monochromator and RCA model 8852 PMT for monochromatic detection. TRO spectra derived from this system were constructed by laminating together such decay curves recorded at different λ_{mon}. A second system recorded broad band spectra at specific delay times using an Acton Research Corp. SpectraPro-275 spectrograph and a Princeton Instruments LN2 cooled 1024EUV CCD camera.

3. Results and discussion

The electronic spectrum of Roussin's red salt displays a strong absorption band centered at 374 nm ($\varepsilon = 1.04 \times 10^4$ M^{-1} cm^{-1}), which tails far into the visible ($\varepsilon = 530$ M^{-1} cm^{-1} at 550 nm). Other apparent maxima appear at 242 nm (2.8×10^4 $M^{-1}cm^{-1}$) and 314 nm (0.85×10^4 M^{-1} cm^{-1}) (Fig. 1). The position and strength of these bands are not changed significantly upon alteration of solvent or cation. EHMO calculations indicate that the frontier orbitals of $Fe_2S_2(NO)_4^{2-}$ are largely confined to the Fe_2S_2 core [8], although given the photoreactivity, it seems likely that the RRS LUMO may have some Fe–NO antibonding character [1].

3.1. Flash photolysis experiment

Preliminary TRO experiments with **RRS** in aerated solutions were compromised by the net photochemistry. In order to avoid flash photolysis of secondary products, fresh solutions of **RRS** (3.0 ml) were flashed once (one transient trace taken) then shaken between each laser excitation pulse (355 nm). Each sample was flashed a maximum of five times before the solution was replaced.

When such studies were carried out in aerated, aqueous solutions, flash photolysis of **RRS** (20–200 μM) led to strong transient bleaching (TB) between 350 and 470 nm. Decay of this first transient $\mathbf{I_i}$ could be fit to simple exponential decay ($k_{obs} = (2.2 \pm 0.2) \times 10^4$ s^{-1}) (Fig. 2). At λ_{mon} less than 470 nm, there was a long-lived (> 50 ms) residual TB, while above 470 nm, the initial bleach evolved into a transient absorbance (TA) (Fig. 2) with the same long lifetime as the residual TB seen at shorter λ_{mon} Although, too long (> 50 ms) to determine in the laser

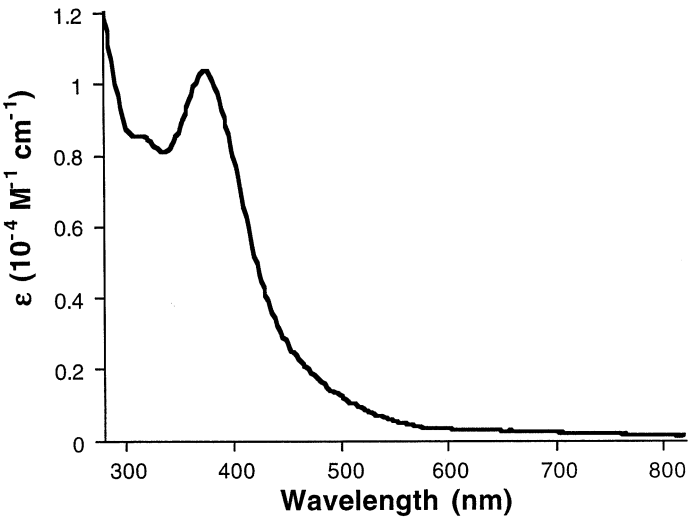

Fig. 1. UV–vis spectrum of $Na_2[Fe_2S_2(NO)_4]$ solution in H_2O.

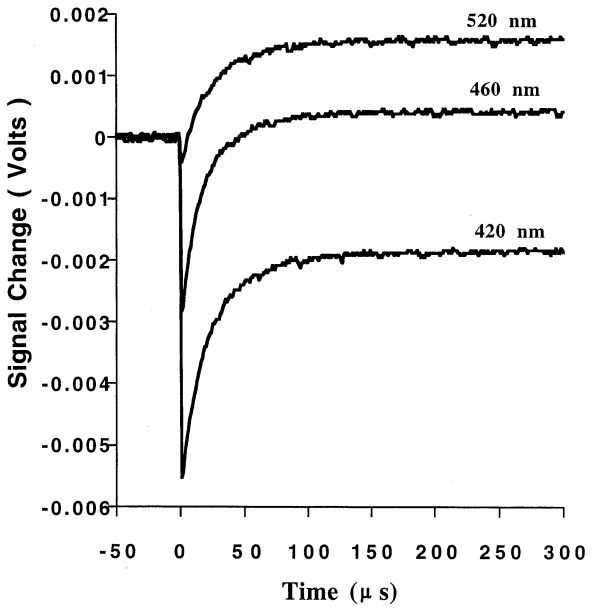

Fig. 2. Transient signal changes upon flash photolysis of $Na_2[Fe_2S_2(NO)_4]$ solution (40 μM) in aerated water, 296 K. Various λ_{mon} ($\lambda_{irr} = 355$ nm). Signal changes rather than absorption changes are used to emphasize qualitative differences.

flash experiment, the lifetime of this second species ($\mathbf{I_{ii}}$) was too short (< 1 min) to observe by conventional spectroscopic methods. Flash photolysis experiments on aqueous **RRS** solutions using CCD camera detection gave TRO difference spectra matching absorbance changes seen in single wavelength experiments (Fig. 3).

When the analogous experiments were carried out in aqueous solutions which had been equilibrated with pure O_2 (1 atm), the rate of the transient decay increased nearly fourfold ($k_{obs} = (7.9 \pm 0.4) \times 10^4\ s^{-1}$). Furthermore, about three times as much of the long-lived intermediate was formed under O_2 than in air equilibrated water.

The pattern was different for flash photolysis of *deaerated* aqueous **RRS** solutions. The first intermediate $\mathbf{I_i}$ was formed in good yield, but the TB decayed back to the original baseline, so $\mathbf{I_{ii}}$ was not formed in concentrations sufficient to be observable (Fig. 4). The decays were much slower than in air and could be fitted to a second-order rate equation. These observations can be counterpoised against the continuous photolysis experiments described in Section 1 where net photoreaction of **RRS** to give **RBS** was largely, but not entirely, suppressed in deoxygenated solutions [1]. Neither raising the ionic strength (to 3 M with NaCl) nor changing the buffered pH from 6 to 10 affected the lifetimes of $\mathbf{I_i}$ in deaerated aqueous solutions. Furthermore, no alterations to rates were seen upon varying [**RRS**] over the range 20–150 μM or by adding Na_2S (up to 100 mM).

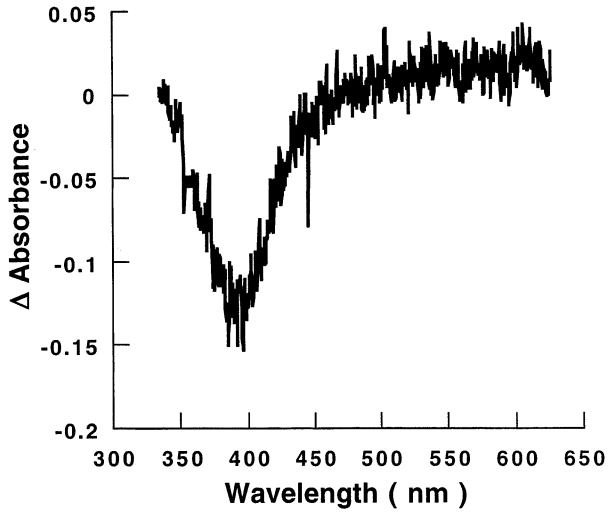

Fig. 3. UV–vis transient absorption by CCD camera. Red Roussin's salt (60 μM) aqueous solution. Gate width = 10 μs, Gate delay = 20 ns; $\lambda_{pump} = 355$ nm. ΔAbs is referenced to the initial absorbance prior to the flash.

The lower limit for a quantum yield of forming a bleached transient in the flash photolysis experiment can be estimated by assuming that the pulse excites all molecules in the observation volume and that the transients formed have no

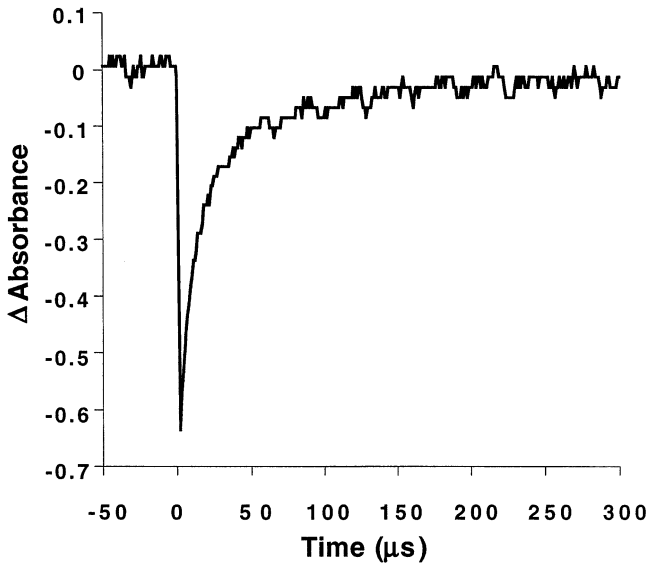

Fig. 4. Transient absorption upon flash photolysis of $Na_2[Fe_2S_2(NO)_4]$ solution (40 μM) in water under argon, 296 K ($\lambda_{mon} = 420$ nm; $\lambda_{irr} = 355$ nm).

absorbance at λ_{mon}, i.e. $\Delta\varepsilon = -\varepsilon_{parent}$. In this manner the bleach monitored at 420 nm was used to estimate a ϕ_l (lower limit) value of 0.4. The magnitude of the prompt transient bleaching, i.e. ϕ_i, was independent of $[O_2]$ in contrast to the kinetics of $\mathbf{I_i}$ decay and the residual absorbances seen.

Flash photolysis of **RRS** in aerated acetonitrile showed absorbance changes analogous to those in aqueous solutions, suggesting that the same intermediate $\mathbf{I_i}$ is formed and undergoes reaction with dioxygen to give $\mathbf{I_{ii}}$ in both solvents. Again, the decay of the first transient was exponential ($k_{obs} = (9.9 \pm 0.6) \times 10^4$ s^{-1} at 295 K) and led to long-lived absorbance changes. The faster rate may reflect solvent effects on the kinetics of $\mathbf{I_i}$, but it should be emphasized that O_2 solubility is considerably higher in acetonitrile (8.1×10^{-3} mol l^{-1} atm^{-1}) than in water (1.3×10^{-3} mol l^{-1} atm^{-1}) [9]. Thus, given the observed sensitivity of the kinetics of $\mathbf{I_i}$ decay to $[O_2]$, a faster rate of decay might have been expected regardless of specific solvent effects. Notably, quantum yields for **RRS** photoreaction under CW photolysis are twofold larger in air equilibrated acetonitrile than in water under analogous conditions [1].

Flash photolysis in deoxygenated acetonitrile led to transient optical spectral changes consistent with formation of $\mathbf{I_i}$. However, the temporal absorbance changes were again best fit to a second-order rate equation and decayed to the original baseline with little indication of other intermediates or product(s) within the sensitivity of the TRO instrumentation.

Aqueous solutions of **RRS** react thermally with NO at rates sufficient to prevent determining [NO] effects on quantum yields measured by CW photolysis experiments. However, the thermal reaction is sufficiently slow at low [NO] that solutions could be prepared and the effect(s) of added NO on transient decay rates qualitatively probed by flash photolysis. This was done in deaerated solution which had been equilibrated with a NO partial pressure (P_{NO}) of 60 torr ([NO] = 140 μM). Under these conditions, the decay rate of $\mathbf{I_i}$ was greatly increased, and temporal absorbance changes could be fit to an exponential function (Fig. 4). The k_{obs} value measured thus ($(1.3 \pm 0.1) \times 10^5$ s^{-1}) translates into a second rate constant $k_{NO} = (9.1 \pm 0.7) \times 10^8$ M^{-1} s^{-1}, if a second-order reaction of $\mathbf{I_i}$ with NO is assumed. -Fig. 5 also shows that while the magnitude of long-lived absorbance change decreased substantially from that seen in aerated solution, the residual ΔAbs was larger than that seen in deoxygenated solutions without added NO.

The flash photolysis data can be interpreted in terms of the reactions outlined in Scheme 1 in which the first intermediate $\mathbf{I_i}$ is generated in high yield by photodissociation of nitric oxide. Subsequently, $\mathbf{I_i}$ is trapped competitively by NO to regenerate **RRS** or by O_2 to give the second intermediate $\mathbf{I_{ii}}$ (the precursor to the eventual product, **RBS**). The reverse reaction back to **RRS** is evidenced by the second-order decay of $\mathbf{I_i}$ in deaerated solution and by the much faster decay when excess NO is present. According to this model, one would not predict the apparent exponential decay of $\mathbf{I_i}$ seen in aerated water, since, under those conditions $\mathbf{I_i}$ is being depleted by the second-order reaction with stoichiometrically formed NO and pseudo-first-order reaction with the excess O_2 present. Notably, the calculated k_{obs} increased, although not linearly, when $[O_2]$ was raised fivefold in going from aerated to

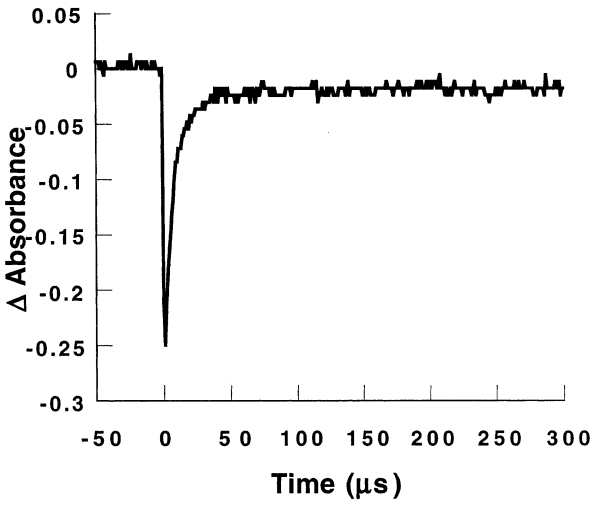

Fig. 5. Transient absorption upon flash photolysis of $Na_2[Fe_2S_2(NO)_4]$ solution (40 μM) in water under 60 torr NO, 296 K ($\lambda_{mon} = 420$ nm; $\lambda_{irr} = 355$ nm).

O_2-equilibrated aqueous solution (both at 1.0 atm). We attribute this behavior to the value of k_{NO} being much larger than that of k_{Ox}. Thus, the second-order reaction with photogenerated NO remains somewhat competitive with O_2 trapping of $\mathbf{I_i}$ in aerated solution. However, if redox trapping of $\mathbf{I_i}$ is assumed to be dominant under pure O_2, the value of k_{Ox} can be estimated as $(\sim 5.7 \pm 0.3) \times 10^7\ M^{-1}\ s^{-1}$.

The kinetics modeling program STELLA II was used to simulate the kinetic flash data under various conditions using Scheme 1 as the model and the values of k_{Ox} and k_{NO} described above. Numerical analysis gave curves that match well with those observed upon flash photolysis under aerated, oxygenated and deoxygenated conditions, including the appearance of exponential decay despite significant contributions from both a pseudo-first-order process and a second-order process.

In order to form **RBS** photochemically, **RRS** must lose NO, combine with another **RRS**, lose sulfide and work out the fate of the extra electron, although not necessarily in that order. The flash data can be reasonably interpreted according to

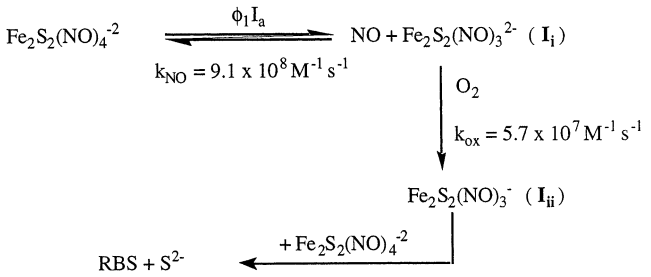

Scheme 1. Roussin's red salt photochemistry observed in flash photolysis.

Scheme 1, particularly with regard to the competitive trapping of $Fe_2S_2(NO)_3^{2-}$ by NO and O_2. Since Φ_{RRS} is insensitive to variations of ionic strength or [**RRS**], dioxygen trapping of $\mathbf{I_i}$ appears to be the limiting step in the eventual formation of the anionic tetranuclear clusters. Thus, the quantum yield is defined by the competitive trapping as indicated in Eq. (2), where $[NO]_{SS}$ is the steady state concentration of nitric oxide under the experimental conditions.

$$\Phi_{RRS} = \frac{\dfrac{-\mathrm{d}[RRS]}{\mathrm{d}t}}{I_a} = \left[\frac{k_{Ox}[O_2]\phi_1}{k_{Ox}[O_2] + k_{NO}[NO]_{SS}}\right] \quad (2)$$

Previous quantum yield determinations under continuous photolysis conditions were made with absorbed light intensities (I_a) approximately constant at 5×10^{-6} einsteins s^{-1} l^{-1}. Under this I_a, the Φ_{RRS} values found were 0.142 ± 0.006 in aerated aqueous solution, independent of λ_{irr}. However, the model described by Scheme 1 suggests that under CW photolysis conditions, Φ_{RRS} will be dependent on I_a in aerated solution, since, in the absence of added NO, the steady state concentrations $[\mathbf{I_i}]_{SS}$ and $[NO]_{SS}$ are both functions of I_a. Thus, at higher intensity, the competitive second-order back-reaction of $\mathbf{I_i}$ with NO is enhanced relative to the pseudo-first-order trapping by O_2, which is present at a constant concentration. At very high I_a, the limit would be $k_{NO}[NO]_{SS} \gg k_{Ox}[O_2]$, at which point $[NO]_{SS}$ can be shown to be proportional to $I_a^{1/2}$, thus Φ_{RRS} would be proportional to $I_a^{-1/2}$. At low I_a, the second limiting condition would be $k_{Ox}[O_2] \gg k_{NO}[NO]_{SS}$, and at this point $\Phi_{RRS} \approx \phi_1$. Obviously, the situation is more complex under nonlimiting conditions.

This proposal was tested by measuring quantum yields at different I_a values. As predicted, Φ_{RRS} values increased as I_a decreased. Table 1 shows that the product $\Phi_{RRS} \times I_a^{1/2}$, while roughly constant, appears to be approaching the second limiting condition at the lowest I_a.

It should be noted that Scheme 1 proposes that $\mathbf{I_{ii}}$ has the formulation $Fe_2S_2(NO)_3^-$. In this context, it is notable that the $Fe_2S_2(NO)_3^-$ ion was observed as a strong peak in electrospray mass spectroscopy experiments on the red salt in aqueous solutions [1], suggesting that such a species may be relatively stable. If $Fe_2S_2(NO)_3^-$ is formed, it must react relatively quickly with a **RRS** ion to give the stable **RBS** product plus S^{2-}. The pathway proposed in Scheme 2 is consistent with

Table 1
Quantum yields for **RRS** photoconversion as a function of absorbed light intensity ($\lambda_{irr} = 365$ nm) in aqueous solution

Medium	I_a[a] (einsteins s^{-1} l^{-1}) ($\times 10^6$)	Φ_{RRS}[b]	$\Phi_{RBS} \times I_a^{1/2}$ ($\times 10^4$)
Aerated H_2O	5.0 ± 0.01	0.142 ± 0.006	3.13
Aerated H_2O	1.4 ± 0.05	0.23 ± 0.1	2.72
Aerated H_2O	0.15 ± 0.2	0.56 ± 0.04	2.17

[a] I_a is the rate of photons absorbed by **RBS**.
[b] $\Phi_{RRS} = (\mathrm{d}[RRS]/\mathrm{d}t)(I_a)^{-1}$.

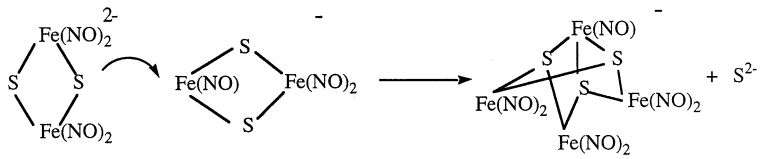

Scheme 2. Proposed step leading to tetrahedral clusters.

the nucleophilicity of the **RRS** anion as illustrated by its reactions with alkyl halides (RX) to form the so-called Roussin's 'esters' of the form $[Fe_2(SR)_2(NO)_4]$ [10].

The flash photolysis behavior of **RRS** has strong analogies to that of the black salt ion **RBS** [11]. In each case the parent anionic iron sulfur nitrosyl cluster undergoes NO photolabilization with high quantum efficiency to form an intermediate which may be trapped competitively by NO to reform the parent ion or by O_2 leading to net photoreactions. For **RRS** in aerated aqueous media and at low to medium light intensities, the back reaction with NO is comparable in magnitude to trapping by O_2. For **RBS** the back reaction with NO is more efficient, thus the quantum yield for net photodecomposition in aqueous aerated solution is much lower ($\Phi_{RBS} = 0.0011$). In both cases, the manner in which dioxygen reacts with the first intermediate is unknown, although it is unlikely to be a simple one-electron oxidation, since the evidence does not support superoxide formation[1].

As noted above, CW photolysis of aerated **RRS** solutions leads to formation of **RBS** regardless of the solvent. When monitored by FTIR spectroscopy in aerated acetonitrile, the only ν_{NO} bands seen were those of the reactant and the final photoproduct (Fig. 6)[2].

3.2. Continuous photolysis experiments in deaerated solutions

In deaerated solvents much longer photolysis times were necessary to achieve significant conversion of **RRS** in keeping with the much lower Φ_{RRS} under those conditions [1]. In deaerated protic solvents such as water or methanol, the optical spectrum changes are consistent with quantitative formation of **RBS** from **RRS**;

[1] The interaction of O_2 and $\mathbf{I_i}$ has superoxide as a potential product. However, superoxide would react quickly with any NO present to produce NO_3^-. Our previous electrochemical detection work demonstrated that the photoconversion of 1 mol of **RRS** to **RBS** is accompanied by the production of 0.5 mol of nitric oxide, as would be predicted in the absence of a NO scavenger such as superoxide. This nitric oxide signal decayed at the same pseudo-second-order rate for autoxidation observed upon injection of standard NO solutions. Furthermore, in electrospray MS experiments upon the aerated, aqueous solutions of **RRS** after photolysis, nitrite was seen as the major product at 46 m/z, with only small signals ($< 10\%$ of nitrite intensity) for nitrate ion at 62 m/z [1]. These data indicate that superoxide is not produced in significant amounts during the photoconversion of **RRS**.

[2] The FTIR spectra of Na^+ and K^+ salts of **RRS** in CH_3CN or CH_3OH are the same. Each displays ν_{NO} bands at 1665 cm^{-1} ($\varepsilon = 8.5 \times 10^3$ M^{-1} cm^{-1}) and 1690 cm^{-1} (8.5×10^3). In the less polar solvents THF and dichloromethane, other ν_{NO} bands (1730–1660 cm^{-1}) are seen, presumably due to greater ion pairing in those solvents.

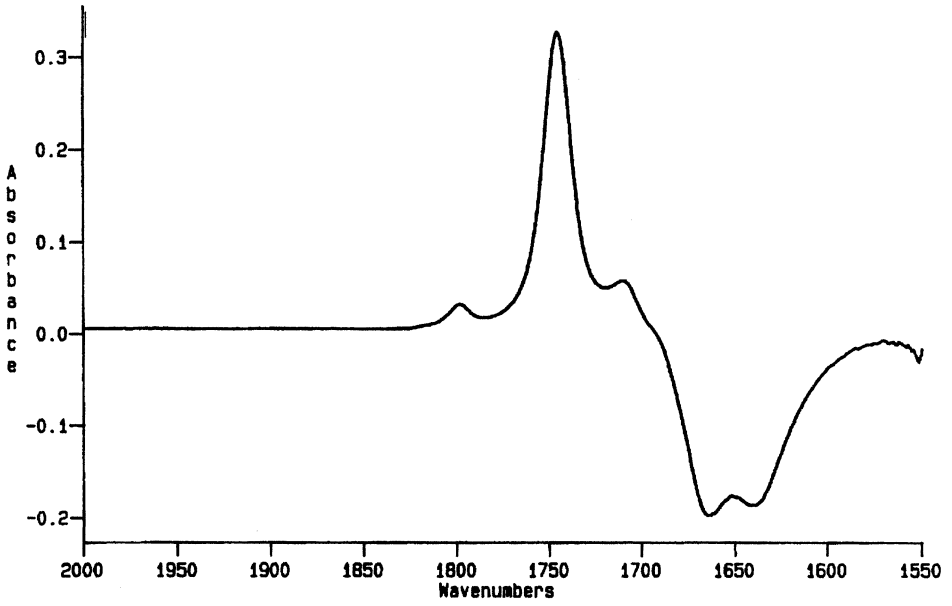

Fig. 6. FTIR spectral changes upon photolysis of $Na_2[Fe_2S_2(NO)_4]$ in aerated CH_3CN ($\lambda_{irr} = 355$ nm). Shown is the difference spectrum relative to that of the initial spectrum before photolysis.

however, in THF or acetonitrile, FTIR spectral changes indicated that disappearance of **RRS** ν_{NO} bands is accompanied by the growth of new ν_{NO} bands at 1747 (m), 1690 (s), 1660 (sh) cm^{-1} (Fig. 7) characteristic of the tetranuclear black salt dianion $Fe_4S_3(NO)_7^{2-}$ (**BSD**) [12], as well as an unidentified band at ca. 1711 cm^{-1}. Upon exposure of these solutions to air, the new ν_{NO} bands disappeared and those of **RBS** appeared (1800 (w), 1745 (s), and 1706 (w) cm^{-1}).

In order to confirm that **BSD** is the above product, $[NEt_4]_2[Fe_4S_3(NO)_7]$ was prepared by Zn/Hg amalgam reduction of $[NEt_4][Fe_4S_3(NO)_7]$ in acetonitrile (under Ar) in the presence of excess $[NEt_4]Br$ [12]. Upon reduction, the color of the solution changed from deep black–green to a brown–black, although the UV–vis spectrum proved only subtly different from that **RBS**. Nevertheless, the FTIR spectrum displayed ν_{NO} bands at 1749 (m), 1690 (s), and 1660 (sh) cm^{-1} matching those of the photolysis product in deoxygenated acetonitrile.

In the absence of O_2, NO is the most likely target for reduction. This would result in formation of the nitroxyl anion, NO^-, which would react further in protic solvents to give nitrous oxide (Eq. (3)). When aqueous **RRS** solutions in evacuated cells were subjected to long-term photolysis at 365 nm, N_2O (above the normal background) was detected by GC analysis of the gas phase above each solution. The strong N_2O peaks increased as the photolysis progressed, consistent with this hypothesis.

$$2NO^- + 2H^+ \rightarrow H_2O + N_2O \quad (3)$$

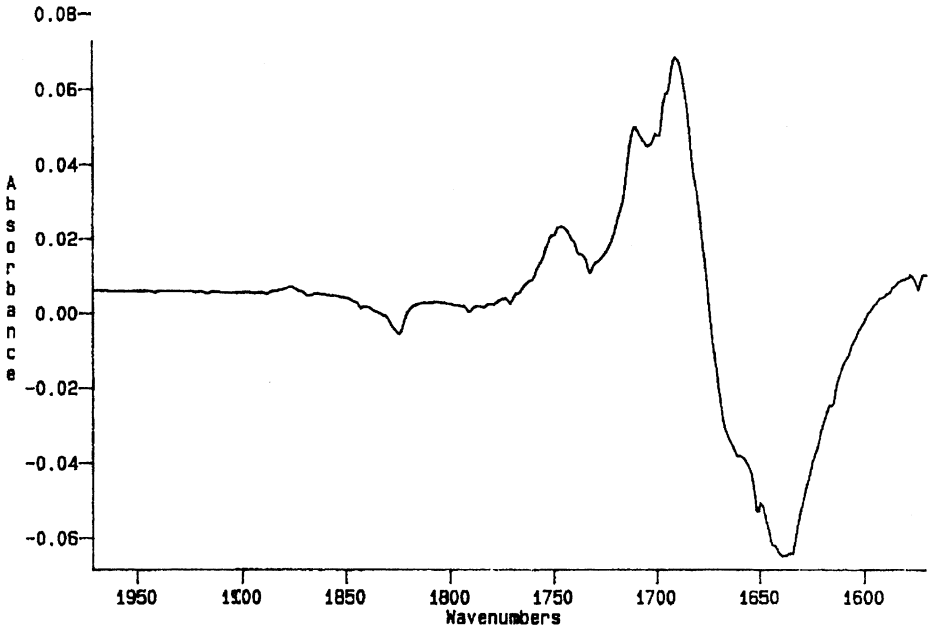

Fig. 7. FTIR spectral changes upon photolysis of $Na_2[Fe_2S_2(NO)_4]$ in deoxygenated CH_3CN ($\lambda_{irr} = 355$ nm).

In order to determine the N_2O product quantitatively, 5.0 ml aliquots of aqueous **RRS** solutions (0.05–0.15 M) were placed in gas-tight photolysis cells with measured total volumes between 20 and 30 ml. The solutions were degassed by four f-p-t cycles, equilibrated with 1.0 atm Ar and the cells sealed. The solutions were then irradiated by the UV–vis output of a 200 W short arc Hg lamp, filtered only for IR radiation. Subsequently, the solutions were diluted 1000-fold by removing 3.0 μl aliquots and injecting these into 3.0 ml of water. This procedure gave concentrations of the iron species amenable to spectrophotometric analysis of the **RRS** to **RBS** conversion. At a point where the predicted formation of N_2O was judged sufficient for analysis (10–50 mmol), a 1.0 ml aliquot of the cell headspace was withdrawn with a gas-tight syringe and analyzed by GC for N_2O with Ar as an internal standard. These experiments showed an average stoichiometry of 0.22 ± 0.03 mol of N_2O per mole of **RRS** converted, consistent with the proposed stoichiometry of Eq. (4)[3].

[3] The photolyses of deaerated concentrated solutions (> 0.01 M) typically would go to ca. 20–30% completion before ceasing to respond significantly to further irradiation. A 1.0 ml aliquot of solution that had reached this point was withdrawn from the airtight cell by syringe. This aliquot was diluted by addition to 9.0 ml of water. The pH of this sample was determined by pH electrode to be 11.3, indicating the pH before dilution to be 12.3, close to the value (12.6) predicted for that particular solution according to Eq. (4). Another solution irradiated to a similar extent was neutralized by injecting 1.0 ml of deaerated 0.16 M HCl solution. Upon further irradiation, the spectral changes resumed. The headspace upon further sampling showed that more N_2O had evolved.

$$2H^+ + 4Fe_2S_2(NO)_4^{2-} \xrightarrow{h\nu} 2Fe_4S_3(NO)_7^- + 2S^{2-} + N_2O + H_2O \quad (4)$$

The potential role of NO as an oxidant in protic media was further supported by experiments in which aliquots of aqueous NO solution (1.9 mM) were injected into a dry acetonitrile solution of the **BSD** salt $[NEt_4]_2[Fe_4S_3(NO)_7]$. This resulted in formation of **RBS**, observed by FTIR and optical spectroscopy, and of N_2O seen qualitatively by FTIR ($\nu_{NO} = 2230\ cm^{-1}$) and by GC. When a 10 ml solution of the black salt dianion (20 mM) in dry acetonitrile was exposed to dry NO at $P_{NO} = 1$ atm, only slight oxidation to the monoanion was seen. Subsequent injection of deoxygenated H_2O (0.1 ml) induced reaction within a few seconds to the monoanion $Fe_4S_3(NO)_7^-$ (confirmed by FTIR). Thus, in deaerated solutions, net photoreaction appears to proceed via formation of **BSD**, which is subsequently oxidized to **RBS** by NO in the protonic medium. However, given the small magnitude of **BSD** formation under those conditions, it seems unlikely that this pathway is the principal one leading to **RBS** formation in aerated media[4].

Continuous photolyses were also performed at low temperatures (-43 to -78°C) in CH_3CN, THF, MeOH and 50/50 MEOH/EtOH. For fluid solutions (both aerated and deaerated), changes in FTIR spectra were analogous to those at ambient temperature. Frozen solutions and glasses displayed no significant spectral changes even upon prolonged photolysis (>1 h). The latter suggests that back reaction of $\mathbf{I_i}$ with NO is very efficient in frozen media, presumably the result of cage recombination.

In summary, there appear to be two independent mechanisms leading to product formation in the photochemistry of **RRS**. The dominant primary photoreaction seen in the flash photolysis experiments is NO labilization to give $\mathbf{I_i}$. The $[O_2]$, [NO] and I_a dependences of this species' lifetime, of $\mathbf{I_{ii}}$ formation, and of the overall quantum yields all point to oxidative trapping of $\mathbf{I_i}$ as the limiting step in the major pathway to **RBS** formation (Scheme 1). However, the oxygen containing product of the oxidative quenching by O_2 has not been identified. A minor pathway leads to formation of the black salt dianion in deaerated, aprotic media. However, since Φ_{RRS} and the lifetime of $\mathbf{I_i}$ are both independent of [**RRS**], reaction of $\mathbf{I_i}$ with the parent ion **RRS** to give **BSD** can not be the major pathway leading to final products in aerated solutions.

Acknowledgements

This work was supported by the National Science Foundation (CHE 9400919 and CHE 9726889) and by a Collaborative UC/Los Alamos Research (CULAR)

[4] An attractive mechanism for **BSD** formation would be the direct reaction of $\mathbf{I_i}$ with the dianion **RRS** to give the **BSD** plus S^{2-} at a rate much slower than the back reaction of $\mathbf{I_i}$ with steady state concentrations of NO. If so, one might expect the Φ_{RRS} values obtained in deaerated solutions to be larger at higher **RRS** concentrations; however, the quantum yield for photoconversion to the black salt dianion in deaerated CH_3CN was found to be independent of [**RRS**] (20–150 μM).

Initiative grant from Los Alamos National Laboratory. TRO experiments were carried out on systems constructed with instrumentation grants from the US Department of Energy University Research Instrumentation Grant Program (No. DE-FG-05-91ER79039) and from the National Science Foundation.

References

[1] J.L. Bourassa, W. DeGraff, S. Kudo, D.A. Wink, J.B. Mitchell, P.C. Ford, J. Am. Chem. Soc. 119 (1997) 2853.
[2] S. Kudo, J.L. Bourassa, S.E. Boggs, Y. Sato, P.C. Ford, Anal. Biochem. 247 (1997) 193.
[3] J.B. Mitchell, D.A. Wink, W. DeGraff, J. Gamson, Cancer Res. 53 (1993) 5845.
[4] D. Seyferth, M.K. Gallagher, M. Cowie, Organometallics 5 (1986) 539.
[5] (a) R. Hintze, P.C. Ford, J. Am. Chem. Soc. 97 (1975) 2664. (b) A.E. Friedman, P.C. Ford, J. Am. Chem. Soc. 111 (1989) 551. (c) R.M. Carlos, M.E. Frink, E. Tfouni, P.C. Ford, Inorg. Chim. Acta 193 (1992) 159. (d) W.T. Boese, P.C. Ford, J. Am. Chem. Soc. 117 (1995) 8381.
[6] (a) J.G. Calvert, J.N. Pitts, Photochemistry, Wiley, New York, 1967, pp. 783–786. (b) G. Malouf, P.C. Ford, J. Am. Chem. Soc. 99 (1977) 7213.
[7] E. Lindsay, P.C. Ford, Inorg. Chim. Acta 242 (1996) 51.
[8] S.-S. Sung, C. Glidewell, A.R. Butler, R. Hoffmann, Inorg. Chem. 24 (1985) 3856.
[9] (a) R. Buttino (ed.), Oxygen and Ozone, IUPAC Solubility Data Series, vol. 7, Pergamon Press, New York, 1981. (b) D.T. Sawyer, G. Chiericato, C.T. Angells, E.J. Nanni Jr., T. Tsuchiya, Anal. Chem. 54 (1982) 1720.
[10] (a) T.B. Rauchfuss, T.D. Weatherill, Inorg. Chem. 21 (1982) 827. (b) D. Seyferth, M.K. Gallagher, M. Cowie, Organometallics 5 (1986) 539.
[11] J.L. Bourassa, B. Lee, S. Bernhard, J. Schoonover, P.C. Ford, Inorg. Chem. 38 (1999) 2947.
[12] S. D'Addario, F. Demartin, L. Grossi, M.C. Iapalucci, F. Laschi, G. Longoni, P. Zanello, Inorg. Chem. 32 (1993) 1153.